I J C T A, 9(38), 2016, pp. 141-148

3D Simulation Study of a Receiver on a Solar Power Tower

M. Hazmoune*,, B. Aour**, A. Bouhallassa*, S. Lecheheb*, M. Laissaoui*, A. Hamidat***

ABSTRACT

In this paper, a detailed model for the three-dimensional (3D) numerical simulation model of solar serial receivers for power tower is presented. The proposed model aims to consider all the major phenomena influencing the performance of a serial receiver, including transfer medium, the heat flux imposed on the wall and the velocity of heat transfer fluid. The software used for this study is ANSYS CFX and an unstructured grid with 825 300 cells. The selection of the standard k–ê turbulent model was used. For the thermal side, we consider only the convection and conduction modes into the receiver, while the effect of radiation is neglected. The simulation results show the influence of different parameters on the temperature field between the input and output of the receiver.

Keywords: 3D-simulation, solar power tower, solar receivers, flow and heat transfer.

1. INTRODUCTION

The solar tower power plants consist of numerous mirrors focus sunlight to a boiler at the top of a tower. Evenly distributed mirrors are called heliostats. Each heliostat is adjustable and individually following incident sunlight and reflects accurately towards the receiver on top of the solar tower. The concentration factor may exceed 1000, which can reach high temperatures ranging from 600°C to 1000°C.

The concentrated energy of the receiver is then directly transferred to the working fluid (steam direct generation of driving a turbine or air heating feeding a gas turbine) is used to heat an intermediate heat transfer fluid. The latter is then sent to a boiler and the steam generated drives turbines. In all cases, the turbines that drive generators used to produce electricity Quoilin Sylvain [1]. Currently, solar tower technologies account for 457 MW operating worldwide, 210 MW under construction and about 6000 MW planned Fang and al [6].

For the production of electricity from solar energy, receivers play an important role in the collection of solar radiation. They transform it into heat by means of a heat transfer fluid to the storage system or the power block. In the last years, many efforts have been focused on the receiver design optimization in order to reduce heat losses and early failure of the tubes, as well as to increase the energy conversion efficiency of the receiver. Lata and al [8], focused their research on the optimization of the diameter and wall thickness of the receiver tubes. In addition, they analyzed different tube materials as nickel. On the contrary, other authors tried modifying the heat transfer fluid (HTF). Jianfeng and al [9], made a numerical analysis using HIATEC, they studied the heat absorption efficiency and heat transfer characteristics of an external receiver under unilateral concentrated solar radiation realizing how the efficiency increases with the incident energy flux and the flow velocity and obtaining value for absorption efficiency between 83 and 90%. A summary of the latest volumetric, particle and tubular

* Centre de Développement des Energies Renouvelables, CDER. BP. 62 Route de l'Observatoire Bouzareah 16340 Algers, Algeria

** Laboratory of Applied Biomechanics and Biomaterials (LABAB), ENP Oran, Algeria, *Email: m.hazmoune@cder.dz*

receivers studied for central receiver (tower) plants is also available, Ho and al [10]. Some recent control methods are discussed in [11-15].

In the present paper, a thermal study of central receiver for a solar power tower plant has been carried out. This is an external receiver that uses water-vapor and molten salt ($NaNO_3$-$NaNO_2$ - KNO_3/ $NaNO_3$- KNO_3 /LiF-NaF-BeF_2) as heat transfer fluid, and detailed information on molten salts properties can be found in Bradshaw and al [7]. The main characteristics of this salt are low vapor pressure, a number of recent projects using molten salt are planned to include an open receiver. Gould and al [3] neither inflammable not explosive, properties desirable for thermal storage. In contrast, it has a great corrosion potential that presents a challenge for the heat exchange in the receiver.

The thermal analysis takes into account circumferential and axial variations of the tube wall temperature. Tube temperature is not circumferentially homogeneous, as in the case of water tube boilers where the wall temperature is approximately the phase change temperature, being the non-uniform interception of solar radiation by the tubes the main cause of the temperature variations in the heat-transfer process.

In this way, the heat flux absorbed by the tubes and the evolution of wall, film and bulk temperatures along the receiver has been calculated. In addition, in order to optimize the design of the receivers and the heliostat field and assure the lifetime of SPT, the thermal stresses of the tubes, the total pressure drop and the thermal efficiency of the receiver, based on the wall temperature of each tube element (and not on the mean wall temperature) have been analyzed. Much work has been done on the receivers; one basic requirement for the design of central receivers using a fluid that may freeze above ambient temperature (e.g. sodium or molten salt) is its self-draining ability [5]. Figures 1 and 2 show respectively the solar tower and solar receiver.

2. GEOMETRY DETAILS

ANSYS CFX software (Version 13) was employed for this study, we made geometry by ANSYS WERKBENCH, the diameter of the receiver pipe selected in this study was D = 2.2 cm, the length was L = 100 cm and the height H = 100 cm, see Figure. 3.

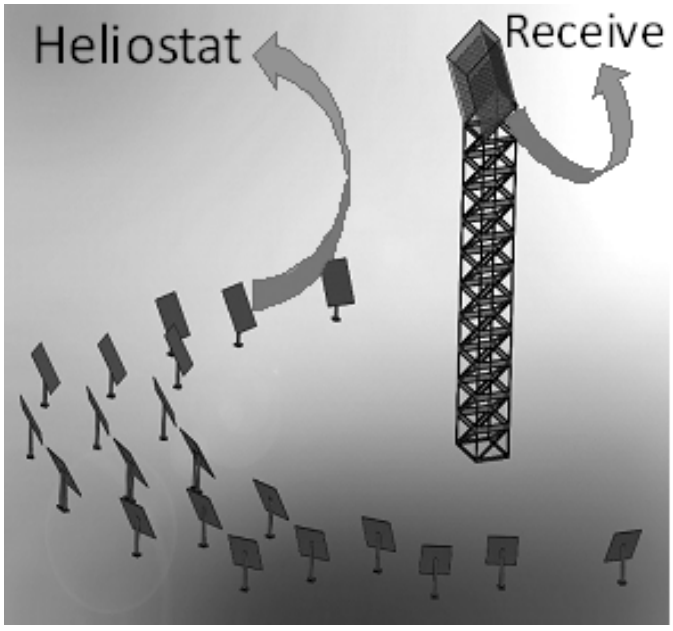

Figure 1: Solar power tower

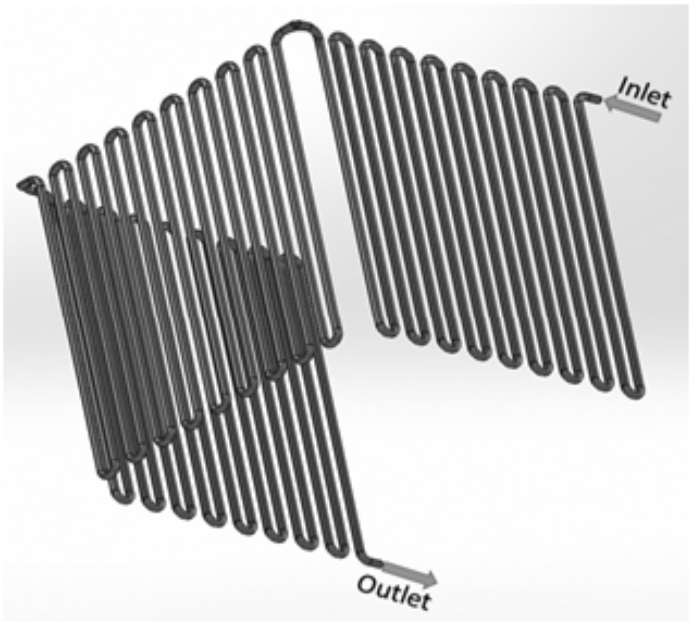

Figure 2: Fluid flow receiver

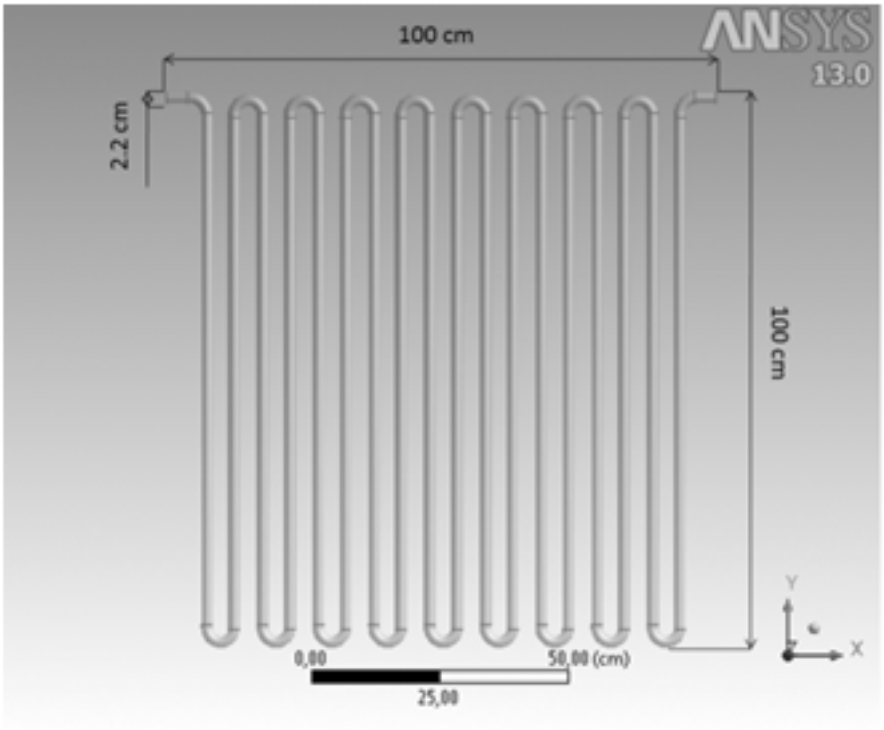

Figure 3: Receiver geometry

3. MESHING

A non-uniform grid system is used to discretize the governing equations, as depicted in Figure 4. It was found that mesh resolution with 825 300 tetrahedral cells gives a good accuracy of results with a relatively reduced CPU time. The choice of this mesh was made by testing: 102 000 cells, 250 456 cells, 562 320 cells, 709 206 cells, 825 300 cells, 1032 256 cells, and 1254 212 cells. Also, we noticed the mesh stability is approximately 825 300 cells.

4. MATHEMATICAL MODEL

The governing equations (mass conservation, momentum and energy), in time averaged tensor notation, for the steady state, are as follow:

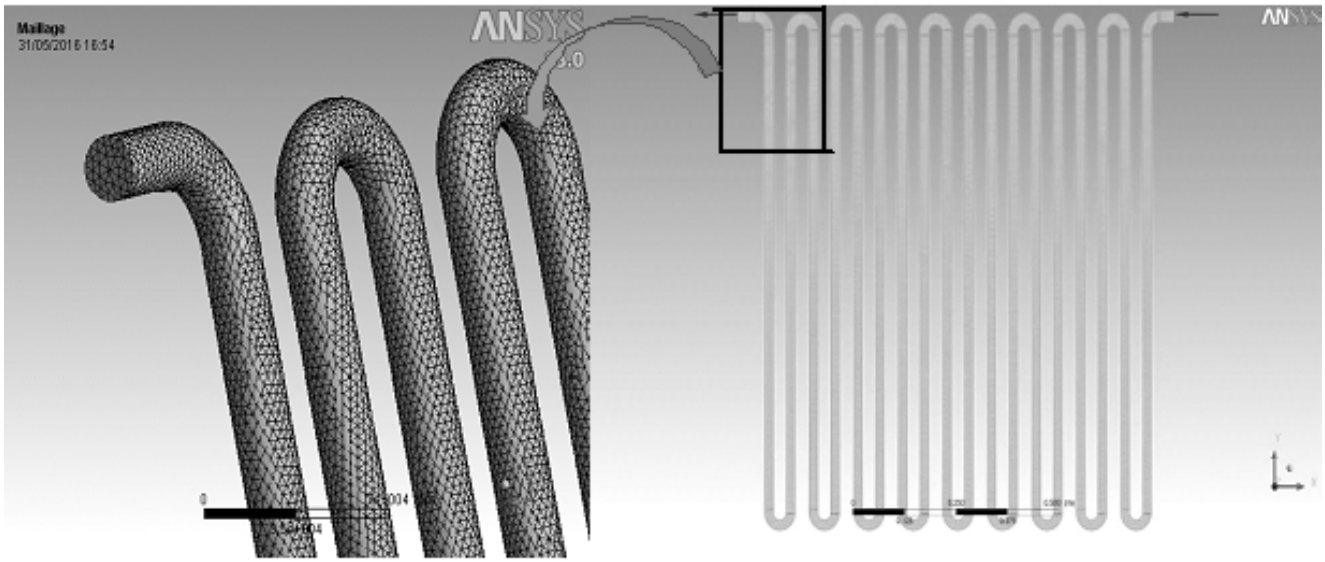

Figure 4: Typical computational grid for numerical analysis

- Continuity:

$$\frac{\partial \overline{u}_t}{\partial x_i} = 0 \tag{1}$$

- Momentum:

$$\rho \overline{u}_j \frac{\partial \overline{u}_t}{\partial x_i} = \frac{\partial \overline{p}}{\partial x_i} + \frac{\partial}{\partial x_j}\left[\mu \frac{\partial \overline{u}_t}{\partial x_j} - \rho \overline{u_t' u'}_j \right] + \rho g i \tag{2}$$

- Energy:

$$\rho \overline{u}_j \frac{\partial \overline{T}}{\partial x_j} = \frac{1}{c_p} \frac{\partial}{\partial x_j}\left[k \frac{\partial \overline{T}}{\partial x_j} - \rho c_p \overline{T' u'}_J \right] \tag{3}$$

4. TURBULENCE

The change of flow direction after leaving the pipe will induce turbulence into the molten salt flow or water-vapor, significantly influencing the heat transfer. Modeling turbulence is thus essential for the simulation. The standard k-ê turbulence model with the standard wall function for the near-wall treatment has been used, i.e. the boundary layer is not resolved by the mesh. A detailed description of the k-å model and its implementation in ANSYS CFX 13 is given by Launder and Spalding (1972) [2] and ANSYS (2009) [4]. In order to better resolve the flow around the outlet of the tube. The turbulent kinetic energy (kt) and the dissipation of the turbulent kinetic energy ([t) are obtained from their transport equations:

- Turbulent kinetic energy (k_t):

$$\rho \overline{u}_J \frac{\partial \overline{k}_t}{\partial x_t} = \frac{\partial}{\partial x_j}\left[\left(\mu + \frac{\mu_t}{\sigma_{kt}} \right) \frac{\partial \overline{k}_t}{\partial xj} \right] + P_{kt} + G_{kt} + \rho_t \tag{4}$$

- Dissipation of the turbulent kinetic energy ([$_t$]):

$$\rho u_J \frac{\partial_t}{\partial x_j} = \frac{\partial}{\partial x_j}\left[\left(\mu + \frac{\mu_t}{\sigma_t} \right) \frac{\partial_t^-}{\partial xj} \right] + C_{1_t} \frac{t}{k}\left[P_{kt} + C_{3_t} G_{kt} \right] - C_{2_t} \rho \frac{\overset{2}{t}}{k_t} \tag{5}$$

5. RESULTS AND DISCUSSION

In this study, flux distribution has been estimated by assuming normal incidence of solar insolation and sun as a point source. Energy balance has been established to calculate temperature distributions over the entire cross-section of receiver pipe at different fluid temperature. These temperature distributions have been fitted and shown in Figures 5 to 8. The temperature between the input and the receiver output given by the dimension relation:

$$Q = \frac{T^4 - T_{\min}^4}{T_{\max}^4 - T_{\min}^4} \tag{6}$$

5.1. Temperature distribution between inlet and outlet of receiver

Figure 5 shows the contours of temperature between inlet and outlet of receiver wall x-axis.

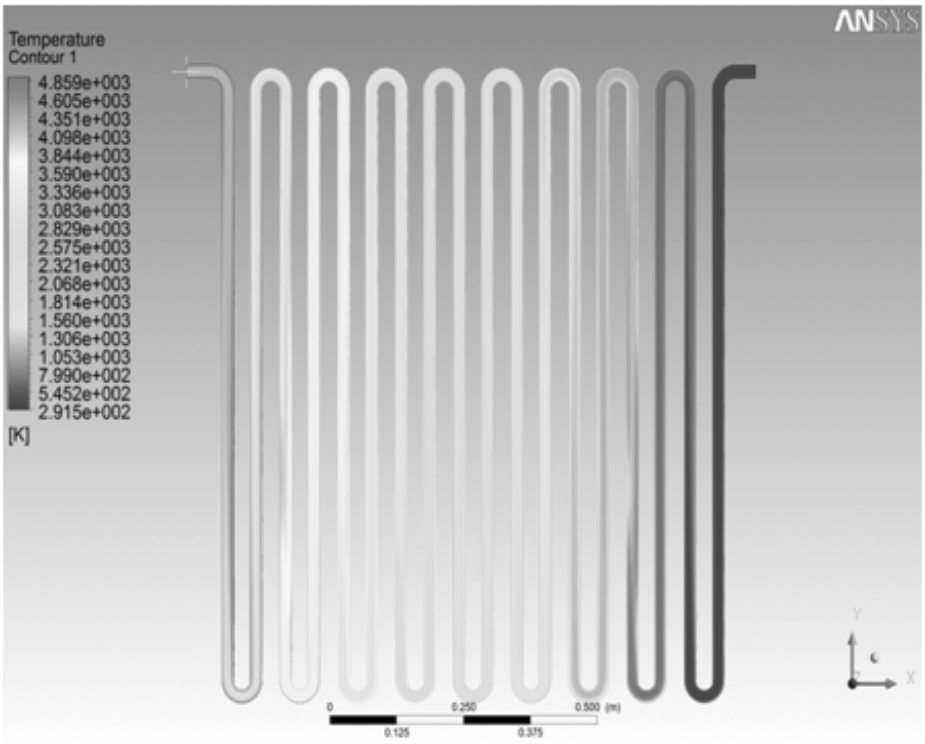

Figure 5: Contours of temperature between inlet and outlet of receiver wall x-axis.

The temperature distribution of the water vapor and the tube wall for velocity 0.1 m/s. The wall temperature distribution between inlet and outlet is uneven due to the non-uniform incident heat flux, in this case. This figure shows that the maximum wall temperature is located on the receiver output, where the incident heat flux is maximum. The temperature difference between the inlet and outlet is very important. The effect of the velocity is clearly visible in figure 5, the heat transfer is enhanced by the velocity, and thus, the maximum value of temperature increases very rapidly between the inlet and outlet of receiver.

5.2. Influence of velocity on the temperature

Figure 6 shows the effects of velocity rates on the outlet temperature.

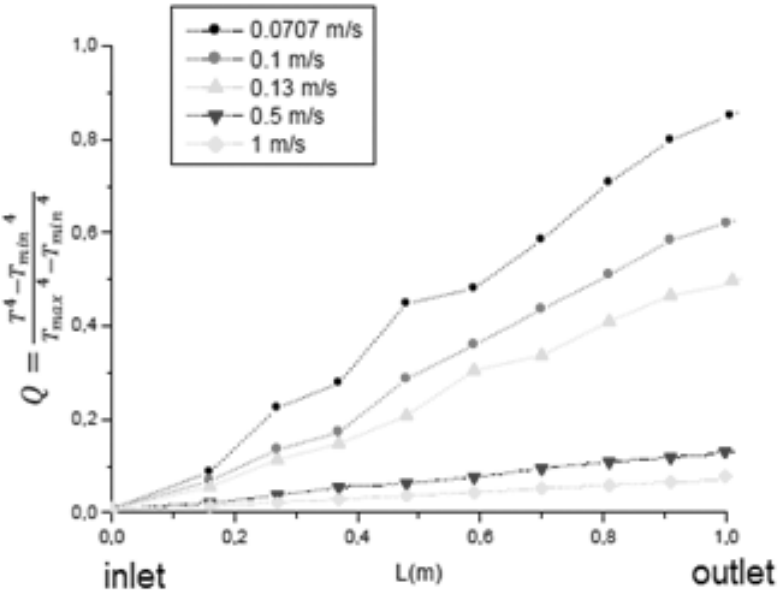

Figure 6: Temperature profile for different axial velocity

The simulated mean temperature profile showed different zones of the receiver: In the inlet a zone where the temperature is equal to the ambient temperature 300 K, and the maximum temperature in outlet on receiver tube. The flow imposed by the heliostats on the receiver wall is 0.5 MW/m2, the fluid used is water-vapor, the pressure at the output is 1 bar, and different velocities at the receiver inlet. In the simulation work, when we increased the velocity in inlet from 0.0707 m/s to 1 m/s, the outlet temperatures increased from 300 K to 706.479 K. A rapid increase caused by the relatively low specific heat capacity of the water-vapor occurs initially, as shown in figure 6. We observe that the increase in velocity at the entrance decreases the temperature at the output that we need to generate the turbine.

5.3. Influence of heat flux

The temperatures profile for different heat flux obtained from ANSYS-CFX software are illustrated in Figure 7.

Lists the outlet temperatures forecasted by the comprehensive simulation model when the average flux incident on the receiver cover ranges from 0.5 MW/m2 to 2 MW/m2. The temperature of exit can be to vary according to the flow of heat imposed on the wall of the receiver, if the average heat flux reaches 1.5 MW/m2 or 2 MW/m2, for a water-vapor velocity than 0.5 m/s. Thus raising the heat flow reflected by many mirrors (heliostats) increases the temperature at the output of receiver.

5.4. Influence of the heat transfer fluid

Figure 8 illustrates the temperature profile with different heat transfer fluid.

This part includes the hydrodynamics of the molten salt and water-vapor flow, the convective heat transfer on the inside and the conduction. Depending on the absorbed heat flux, these transfer mechanisms result in a surface temperature field that significantly influences the thermal emissions. with an axial velocity equal to 0.5 m/s with a heat flux 0.5 W/m2, and a temperature input 503 K to the molten salt and 300 K for water-vapor. In this work, we used different water-vapor fluids and molten salt (NaNO3-NaNO2 -KNO3 / NaNO3- KNO3 / LiF-NaF-BeF2), and according to the results of the numerical simulation and the results

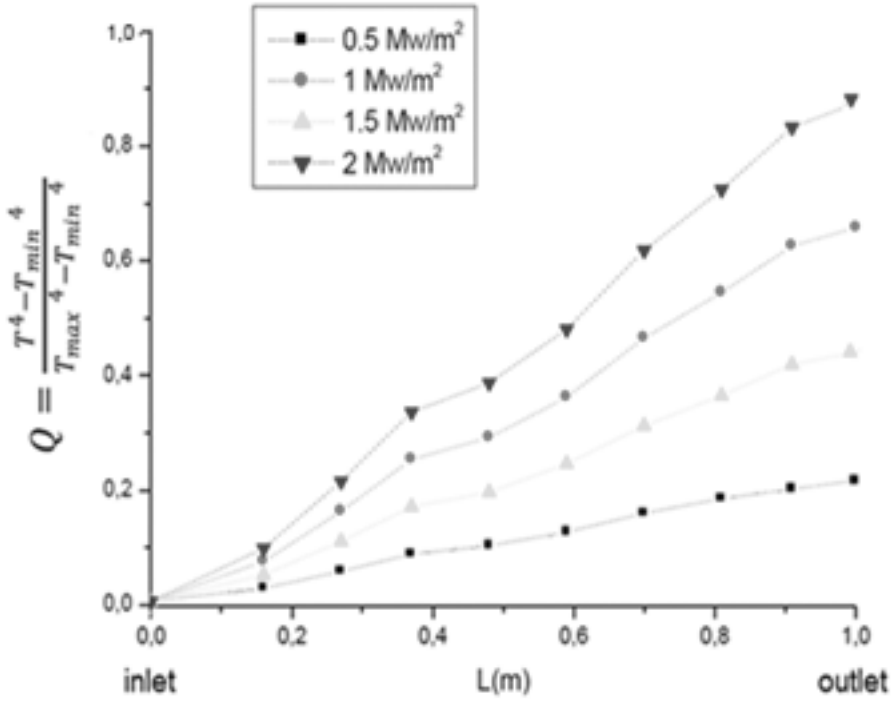

Figure 7: Temperature profile for different heat flux

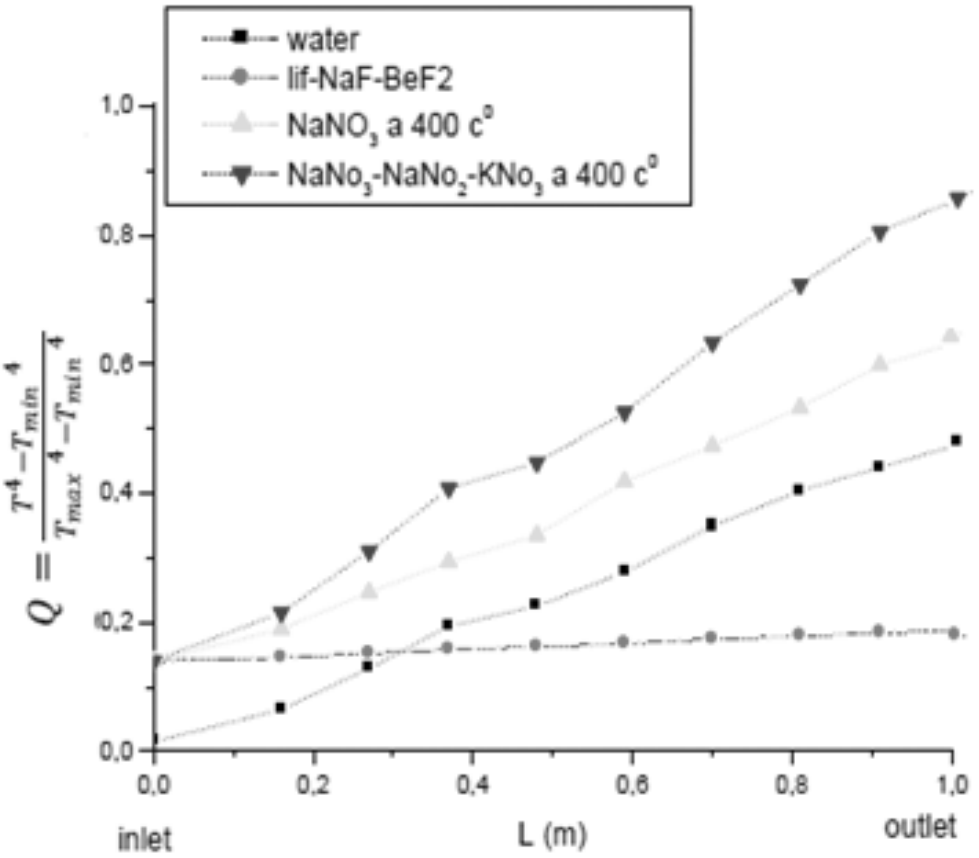

Figure 8: Temperature profile for different heat transfer fluid

of the literature, we noticed that the increase in temperature between the input and the receiver output will be higher with molten salts (NaNO3, NaNO2 -KNO3) that other fluids tested. The molten salt is streaming on the inside of the tubes. This type of receiver is suitable for a surrounding heliostat field, which allows the receiver to be employed in large-scale power plants. The disadvantage of this design is the direct exposure of hot surfaces to the ambiance, to which almost all reflected and emitted radiation is lost. Since natural convection is not restrained by a surrounding structure and wind can directly impinge on the hot absorber tubes and the convective losses are also high.

6. CONCLUSIONS

This work presents a receiver model, in which all the main parameters, namely velocity of flow in inlet, heat flux imposed on the receiver and different heat transfer fluid. The model is able to predict the performance of a serial receiver. This study helps us to choose the best fluid, the fluid velocity in inlet according to turbine that we will use to make solar tower, and heat flow imposed on the receiver that requires us to choose the best site.

Future work should include the validation of the presented model through prototype testing. In addition, other parameters will be tested, such as, the dimensions of the geometry and the coefficients of the radiation transfer.

REFERENCES

[1] Q. Sylvain, "Les Centrales Solaires à Concentration," www.sft.asso.fr/Local/sft/dir/user-3775/documents/actes/journeessft/JSFT-13-6-12/4.pdf, 16/06/2015, 2007.

[2] N.Z. Ince and B.E. Launder, "On the computation of buoyancy driven turbulent flows in rectangular enclosures,"*International Journal of Heat and Fluid Flow*, **10**, 110-117, 1989.

[3] W.R. Gould, "Solarreserve's 565 MW molten salt power towers," Proceedings of the 2011 SolarPACES Conference, 2011.

[4] *ANSYS FLUENT 12.0 Theory Guide*,ANSYS, Inc.,2009.

[5] F.K. Boese, A. Merkel, D. Stahl and H. Stehle,"A consideration of possible receiver designs for solar tower plants,"*Solar Energy*,**26**, 1–7, 1981.

[6] J.B. Fang, J.J. Wei, X.W. Dong and Y.S. Wang, "Thermal performance simulation of a solar cavity receiver under windy conditions. *Solar Energy*,**85**, 126–138, 2011.

[7] R.W. Bradshaw and R.W. Carling, "A review of the chemical and physical properties of molten alkali nitrate salts and their effect on materials used for solar central receivers," *Journal of the Electrochemical Society*, 134 (8), 1080-1088, 1987.

[8] J.M. Lata, M. Rodríguez and A.L. Mónica, "High flux central receivers of molten salts for the new generation of commercial stand-alone solar power plants," *Journal of Solar Energy Engineering*, 130 (2) , Article ID 021002, 2008.

[9] L. Jianfeng, D. Jing and Y. Jianping, "Heat transfer performance of an external receiver pipe under unilateral concentrated solar radiation," *Solar Energy*,**84**, 1879-1887, 2010.

[10] C.K. Ho and B.D. Iverson, "Review of high-temperature central receiver designs for concentrating solar power,"*Renewable and Sustainable Energy Reviews*,**29**, 835-846, 2014.

[11] S. Vaidyanathan and A. Boulkroune, "A novel hyperchaotic system with two quadratic nonlinearities, its analysis and synchronization via integral sliding mode control," *International Journal of Control Theory and Applications*, **9** (1), 321-337, 2016.

[12] S. Sampath, S. Vaidyanathan and V.T. Pham, "A novel 4-D hyperchaotic system with three quadratic nonlinearities, its adaptive control and circuit simulation," *International Journal of Control Theory and Applications*, **9** (1), 339-356, 2016.

[13] S. Vaidyanathan, K. Madhavan and B.A. Idowu, "Backstepping control design for the adaptive stabilization and synchronization of the Pandey jerk chaotic system with unknown parameters", *International Journal of Control Theory and Applications*, **9** (1), 299-319, 2016.

[14] I. Pehlivan, I.M. Moroz and S. Vaidyanathan, "Analysis, synchronization and circuit design of a novel butterfly attractor", *Journal of Sound and Vibration*, **333** (20), 5077-5096, 2014.

[15] A. Sambas, S. Vaidyanathan, M. Mamat, W.S.M. Sanjaya and R.P. Prastio, "Design, analysis of the Genesio-Tesi chaotic system and its electronic experimental implementation", *International Journal of Control Theory and Applications*, **9** (1), 141-149, 2016.